

Measurement of the $^{115}\text{In}(n,\gamma)^{116m}\text{In}$ Reaction Cross-section at the Neutron Energies of 1.12, 2.12, 3.12 and 4.12 MeV

Bioletty Mary LAWRIANIANG, Sylvia BADWAR, Reetuparna GHOSH and Betylda JYRWA
Department of Physics, North Eastern Hill University, Shillong, Meghalaya-793022, India

Vibha VANSOLA
Department of Physics, Faculty of Science, M.S. University, Baroda- 390002, India

Haladhara NAIK* and Ashok GOSWAMI
Radiochemistry Division, Bhabha Atomic Research Centre, Mumbai-400085, India

Yeshwant NAIK and Chandra Shekhar DATRIK
Product Development Division, Bhabha Atomic Research Centre, Mumbai-400085, India

Amit Kumar GUPTA
Nuclear Physics Division, Bhabha Atomic Research Centre, Mumbai-400085, India

Vijay Pal SINGH, Sudir Shibaji POL, Nagaraju Balabekata SUBRAMANYAM, Arun AGARWAL and Pitambar SINGH
Ion Accelerator Development Division, Bhabha Atomic Research Centre, Mumbai-400085, India

(Received 29 April 2015, in final form 3 June 2015)

The $^{115}\text{In}(n,\gamma)^{116m}\text{In}$ reaction cross section at neutron energies of 1.12, 2.12, 3.12 and 4.12 MeV was determined by using an activation and off-line γ -ray spectrometric technique. The mono-energetic neutron energies of 1.12 – 4.12 MeV were generated from the $^7\text{Li}(p,n)$ reaction by using proton beam with energies of 3 and 4 MeV from the folded tandem ion beam accelerator (FOTIA) at Bhabha Atomic Research Centre (BARC) and with energies of 5 and 6 MeV from the Pelletron facility at Tata Institute of Fundamental Research (TIFR), Mumbai. The $^{197}\text{Au}(n,\gamma)^{198}\text{Au}$ reaction cross-section was used as the neutron flux monitor. The $^{115}\text{In}(n,\gamma)^{116m}\text{In}$ reaction cross-sections at neutron energies of 1.12 – 4.12 MeV were compared with the literature data and were found to be in good agreement with one set of data, but not with others. The $^{115}\text{In}(n,\gamma)^{116m}\text{In}$ cross-section was also calculated theoretically by using the computer code TALYS 1.6 and was found to be slightly lower than the experimental data from the present work and the literature.

PACS numbers: 25.85.Ec

Keywords: $^{115}\text{In}(n,\gamma)^{116m}\text{In}$ reaction cross-section, Off-line γ -ray spectrometric technique, $^{197}\text{Au}(n,\gamma)^{198}\text{Au}$ reaction monitor, TALYS 1.6 calculation

DOI: 10.3938/jkps.67.441

I. INTRODUCTION

Nuclear data such as reaction and fission cross-section as well as decay data are important for reactor design. Among these, the neutron-induced reaction cross-sections of structural materials such as Zr, Nb, Fe, Ni and Cr as well as the end beta decay products from fission products are important from the point of neutron economy of the reactor. In particular stable fission

products such as In, Cd, and rare earths such as Sm and Gd have sufficient neutron absorption cross-sections for thermal neutron energy [1]. However, in a reactor the neutron spectrum has energies from thermal to 15 MeV. Thus, knowledge of the reaction cross section of the neutron absorbing materials at different neutron energies is very important. ^{115}In is a stable end product of an isobaric mass chain of symmetric fission products with mass number 115. Natural In has ^{115}In with an isotopic abundance of 95.71%. In addition, the $^{115}\text{In}(n,n')^{115m}\text{In}$ reaction cross section is used as a flux monitor for neutrons with medium energies from 1.5 to 10 MeV. During

*E-mail: naikhbar@yahoo.com

the $^{115}\text{In}(n,n')^{115m}\text{In}$ reaction, the $^{115}\text{In}(n,\gamma)^{116m}\text{In}$ reaction also takes place at lower neutron energies. The $^{115}\text{In}(n,n')^{115m}\text{In}$ reaction cross section data over a wide range of neutron energies are compiled in EXFOR [2] and are consistent with each other. On the other hand, the $^{115}\text{In}(n,\gamma)^{116m}\text{In}$ reaction cross section data for neutron energies from 0.025 eV to 7.66 MeV and around 14 MeV have been determined by various authors [3–33] by using activation and different counting techniques. However, the $^{115}\text{In}(n,\gamma)^{116m}\text{In}$ reaction cross sections for the neutron energies of 0.46- to 4.5-MeV are not consistent with each other and follow two different trends.

In view of the above, in the present work, we have determined the $^{115}\text{In}(n,\gamma)^{116m}\text{In}$ reaction cross section at neutron energies of 1.12, 2.12, 3.12 and 4.12 MeV by using the off-line gamma spectrometric technique. The $^{197}\text{Au}(n,\gamma)^{198}\text{Au}$ reaction cross section was used as the neutron flux monitor. The $^{115}\text{In}(n,\gamma)^{116m}\text{In}$ cross section as a function of neutron energy was also calculated theoretically by using the computer code TALYS 1.6 [34], and the results were compared with the experimental data of present work and literature data to look for the discrepancies.

II. EXPERIMENTAL DETAILS

For the measurement of the $^{115}\text{In}(n,\gamma)^{116m}\text{In}$ reaction cross sections, experiments were carried out with four different neutron energies at two different accelerators. The experimental work consists of two steps: (i) neutrons beam production and (ii) irradiation of the samples and gamma-ray spectrometric analysis.

1. Neutrons Beam Production

The neutron energies of 1.12, 2.12, 3.12 and 4.12 MeV were produced from the $^7\text{Li}(p,n)^7\text{Be}$ reaction by using proton beams with energies of 3, 4, 5, and 6 MeV [35]. The neutron energies of 1.12 and 2.12 MeV were produced by using the folded tandem ion beam accelerator (FOTIA) at the Van-de-Graff, BARC, Mumbai. A circular LiF pellet of 1-cm diameter and 3-mm thickness was used for neutron production. It was fixed on a stand at an angle of 0° relative to the beam's exit window. For the production of the 1.12 and the 2.12 MeV neutron beams, proton beams with energies of 3 and 4 MeV from the ion beam accelerator were used. A beam collimator of 10-mm in diameter was placed before the target. The current of the incident proton beam during the irradiations was 100 nA for both the 3- and the 4-MeV proton beams, respectively. A 3-mm-thick LiF pellet was sufficient to stop the 3- and the 4-MeV proton beams.

The neutron energies of 3.12 and 4.12 MeV were produced at the 14 UD BARC-TIFR Pelletron facility at

Tata Institute of Fundamental Research (TIFR), Mumbai. The neutrons beam were also generated from the $^7\text{Li}(p,n)^7\text{Be}$ reaction caused by 5- and 6-MeV proton beams from the Pelletron facility impinging on a lithium metal target [35]. These runs were carried out at 6-m height above the analyzing magnet of the Pelletron facility in order that the maximum proton current from the accelerator be utilized [35]. At this port, the terminal voltage was regulated by the generating voltage mode (GVM) caused by the terminal potential stabilizer. Further, we used a beam collimator of 6-mm diameter before the target. The lithium foil used for neutron production was made up of natural lithium with a thickness of 3.7 mg/cm² sandwiched between two tantalum foils of different thicknesses. The maximum energy degradation of the proton beam in the thin lithium metal foil was 0.13 MeV [36]. The front tantalum foil facing the proton beam was the thinner one (3.9 mg/cm²), in which the degradation of proton energy was 50 to 85 keV [36]. On the other hand, the back tantalum foil (beam stopper) was the thicker one (0.025 mm) and was used to stop the proton beam. The current of the incident proton beam during the irradiations was 50 nA at 5 MeV and 60 nA at 6 MeV.

The uncertainties in the above-mentioned neutron energies were calculated as follows: The Q-value for the $^7\text{Li}(p,n)^7\text{Be}$ reaction relative to the ground state is -1.644 MeV whereas the first excited state is 0.431 MeV above the ground state, leading to an average Q-value of -1.868 MeV [37–39]. The threshold value of the $^7\text{Li}(p,n)$ reaction relative to the ground state of ^7Be is 1.881 MeV. Thus, for the proton energies of 3, 4, 5 and 6 MeV, the resulting peak energies of the first group of neutrons (n_0) are 1.12, 2.12, 3.12 and 4.12 MeV, respectively. The corresponding neutron energies of the second group of neutrons (n_1) for the first excited state of ^7Be are 0.63, 1.63, 2.63 and 3.63 MeV, respectively. This is due to the fact that above proton energy of 2.37 MeV, the n_1 group of neutrons is also produced [37–39]. However, the contribution from the n_1 group of neutrons is negligible for the proton energies of 6 MeV. Thus, the energies of the emitted neutrons under the main peak were estimated to be 1.12 ± 0.11 , 2.12 ± 0.15 , 3.12 ± 0.21 , and 4.12 ± 0.22 MeV, respectively. The energy degradation of the proton beam within the lithium metal foil might cause an additional uncertainty. However, that uncertainty was less prominent than the energy spread due to the different population of the n_0 and the n_1 groups of neutrons.

2. Irradiation of Samples and Gamma-ray Spectrometry

In the first experiment at the FOTIA at Van-de-Graff, BARC, two different sets of samples were made. An In metal foil of about 98.8 – 163.7 mg with a purity $\sim 99.99\%$ was wrapped with 0.025-mm-thick Al foil. Similarly, 52.7

Table 1. Nuclear spectroscopic data for the radionuclides from the $^{197}\text{Au}(n,\gamma)^{198m,g}\text{Au}$ and the $^{115}\text{In}(n,\gamma)^{116m,g}\text{In}$ reactions used in the calculation from Ref. 40. The bold numbers are the γ -ray energies, whose activities were used in the calculation.

Nuclide	Spin Parity	Half-life	Decay mode	γ -ray energy (keV)	γ -ray intensity (%)
^{198g}Au	2^-	2.6948 d	β^- (100%)	411.8	95.62
				675.88	0.802
				1087.68	0.1589
^{198m}Au	12^-	2.272 d	IT(100%)	97.21	69.0
				115.2	0.04
				180.30	49.0
				204.10	39.0
				214.89	77.3
				333.82	18.0
^{116g}In	1^+	14.10 sec	β^- (99.98%) ε (0.02%)	818.7	0.0143
				1293.4	1.30
$^{116m1}\text{In}$	5^+	54.29 min	β^- (100%)	138.29	3.7
				416.90	27.2
				818.68	12.13
				1097.28	58.5
				1293.56	84.8
				1507.59	9.92
				1752.50	2.36
$^{116m2}\text{In}$	8^-	2.18 sec		2112.29	15.09

– 59.1 mg of Au metal foil was wrapped with 0.025-mm-thick Al foil to prevent contamination from one to the other. The $^{197}\text{Au}(n,\gamma)^{198g}\text{Au}$ reaction of the Au metal foil was used as a neutron flux monitor. Two sets of Al-wrapped Au and In metal stacked samples were made for two different irradiations. The Au-In stack was wrapped with additional Al foil and kept at a distance of 3-mm behind the LiF target. The stacks of samples were irradiated one set at a time with the neutron beam energies of 1.12 and 2.12 MeV at FOTIA, BARC, Mumbai. The irradiation time was 8.6 h for the neutron energy of 1.12 MeV and 5.6 h for 2.12 MeV.

For the second experiment at BARC-TIFR Pelletron facility at TIFR, Mumbai, two separate sets of samples were also made. In metal foil of about 58.1 – 64.3 mg was wrapped with 0.025-mm-thick Al foil. Similarly, 59 – 59.4 mg of Au metal foil was wrapped separately with 0.025-mm-thick Al foil. Then, two different sets of Al-wrapped In and Au stacks were made for different irradiations at neutron energies of 3.12 and 4.12 MeV, respectively. The individual stacks of In-Au samples were additionally wrapped with two different Al foils. The In-Au stack was mounted at an angle of 0° with respect to the proton beam's direction at a distance of 2.1 cm behind the Ta-Li-Ta stack [38]. Schematic diagrams of the Ta-Li-Ta stack and the In-Au stack are given in Fig. 1. The samples were irradiated one set at a time with neu-

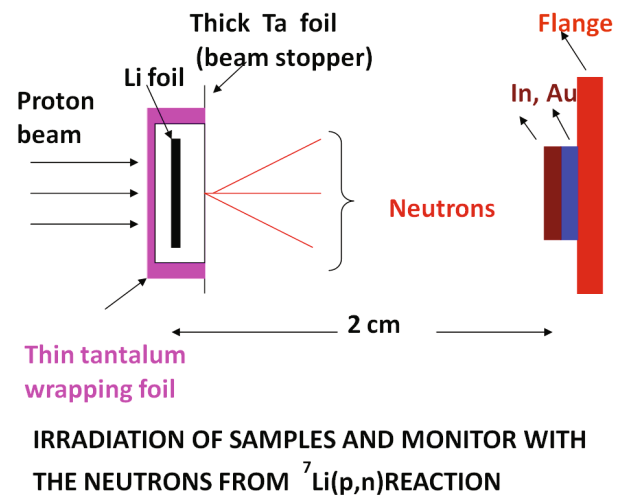


Fig. 1. (Color online) Schematic diagrams showing the arrangements used for the neutron irradiation.

tron beam energies of 3.12 and 4.12 MeV, respectively. The irradiation time was 11.8 h for the neutron energy of 3.12 MeV and 13.4 h for 4.12 MeV.

The irradiated samples of In and Au from the above experiments were cooled for 0.7 – 1.25 h and 2.3 – 19 h, respectively. Then, the γ -ray counting of the samples was done by using a pre-calibrated 80-cc HPGe detector

Table 2. $^{115}\text{In}(n,g)^{116m}\text{In}$ and $^{197}\text{Au}(n,\gamma)^{198g}\text{Au}$ reaction cross-sections at different neutron energies. The reaction cross-sections (σ_R) are within the neutron energies of $^A E_n = 1.014 - 1.232$ MeV and $^B E_n = 2.0 - 2.25$ MeV.

Neutron energy (MeV)	$^{197}\text{Au}(n,\gamma)^{198g}\text{Au}$ cross-section (σ_R) (mb) [Ref.]	Neutron Flux = $\times 10^7$ (n/cm ² s)	$^{115}\text{In}(n,\gamma)^{116m1}\text{In}$ cross-section (σ_R) (mb)		
			Present work	Literature [Ref.]	TALYS 1.6 [34]
1.12 ± 0.12	90.98 ^A [42, 45]	0.628 ± 0.009	271.331 ± 3.374		146.588
	77.552 [47]	0.737 ± 0.016	231.285 ± 2.876		
	78.234 [48]	0.730 ± 0.015	233.318 ± 2.901		
1.17				262.91 ± 28.61 [14]	
2.12 ± 0.15	49.70 ^B [45]	1.955 ± 0.013	120.412 ± 1.631		74.824
	47.347 [47]	2.052 ± 0.014	114.711 ± 1.554		
	50.712 [48]	1.916 ± 0.013	122.864 ± 1.664		
2.16				126.00 ± 6.80 [25]	
3.12 ± 0.21	22.712 [47]	2.334 ± 0.140	41.348 ± 0.538		30.612
	18.558 [48]	1.957 ± 0.117	49.247 ± 0.641		
3.17				39.00 ± 8.20 [25]	
				37.00 ± 4.00 [28]	
3.115				89.00 [27]	
4.12 ± 0.22	11.490 [47]	3.458 ± 0.173	17.839 ± 2.469		13.562
	11.637 [48]	3.401 ± 0.169	18.280 ± 2.511		
4.06				20.40 ± 8.00 [25]	
4.159				40.80 [27]	
4.13				15.40 ± 2.40 [28]	

coupled to a PC-based 4094 channel analyzer. A ^{152}Eu standard source was used for the energy and efficiency calibration. The resolution of the detector system during counting was 2-keV for the 1332-keV gamma-ray of ^{60}Co . A typical gamma-ray spectrum for the irradiated In foil is given in Fig. 2.

III. DATA ANALYSIS

The $^{197}\text{Au}(n,\gamma)^{198g}\text{Au}$ reaction was used as the neutron flux monitor. From the photopeak activity (A_{obs}) of the 412.8-keV γ -ray of ^{198g}Au , the neutron flux (Φ) was obtained by using the following equation [35]:

$$A_{\text{obs}}(CL/LT) = N\sigma_R\Phi I_\gamma \varepsilon (1 - \exp(-\lambda t)) \times \exp(-\lambda T) \times (1 - \exp(\lambda CL))/\lambda, \quad (1)$$

where N is the number of target atoms and σ_R is the cross section of the $^{197}\text{Au}(n,\gamma)^{198g}\text{Au}$ reaction, λ is the decay constant ($\lambda = \ln 2/T_{1/2}$) of the reaction product of interest with a half-life = $T_{1/2}$, I_γ is the branching intensity of the 412.8-keV γ -ray of ^{198g}Au [40], and ε is its detection efficiency. t , T , CL and LT are the irradiation, cooling, clock and live times, respectively.

The cross section of the $^{197}\text{Au}(n,\gamma)^{198g}\text{Au}$ reaction are available in literature [41–46] for the neutron energy from

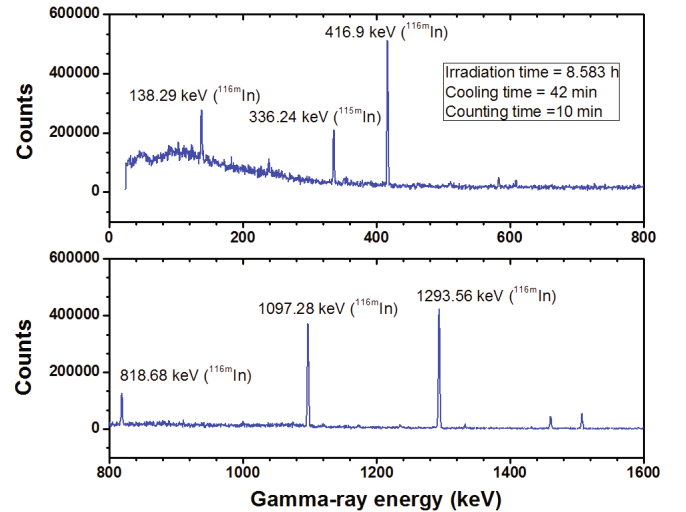


Fig. 2. (Color online) Gamma-ray spectrum of an irradiated ^{nat}In foil with a neutron energy of 1.12 MeV: irradiation time = 8.583 h, cooling time = 42 min, and counting time = 10 min.

0.025 eV to 2.2 MeV and at 14.8 MeV. Thus, for the flux calculation, the $^{197}\text{Au}(n,\gamma)^{198g}\text{Au}$ reaction cross sections from the literature [42,45] were used for neutron energies of 1.12 and 2.12 MeV. However, the $^{197}\text{Au}(n,\gamma)^{198g}\text{Au}$ reaction cross sections available in the literature [42,45]

are for neutron energies of 1.014 and 1.232 MeV, as well as at 2.0 and 2.5 MeV. Thus, at the exact neutron energies of 1.12 and 2.12 MeV, the $^{197}\text{Au}(n,\gamma)^{198g}\text{Au}$ reaction cross sections can be obtained by interpolation from the literature data [42,45]. For comparison, the evaluated $^{197}\text{Au}(n,\gamma)^{198g}\text{Au}$ reaction cross sections from the ENDF/B-VII.1 [47] and the JENDL-4.0 [48] data at the exact neutron energies of 1.12 and 2.12 MeV were also interpolated and used for the flux calculation. No experimental $^{197}\text{Au}(n,\gamma)^{198g}\text{Au}$ reaction cross section data are available for the neutron energies from 2.2 and 14.8 MeV in the literature. Thus, for the exact neutron energies of 3.12 and 4.12 MeV, the $^{197}\text{Au}(n,\gamma)^{198g}\text{Au}$ reaction cross section from ENDF/B-VII.1 [47] and JENDL-4.0 [48] data were interpolated and used for the flux calculation. This was justified because the experimental $^{197}\text{Au}(n,\gamma)^{198g}\text{Au}$ reaction cross sections at neutron energies of 1.12 and 2.12 MeV from the literature [42,45] are comparable to the evaluated data of ENDF/B-VII.1 [47] and JENDL-4.0 [48]. The neutron fluxes obtained from the method describe above were used in rearranged Eq. (1) to calculate the $^{115}\text{In}(n,\gamma)^{116m}\text{In}$ reaction cross section by using the photopeak activities of the 138.33-, 416.86-, 818.72-, 1097.33- and 1293.56-keV γ -lines of ^{116m}In . The nuclear spectroscopic data used in the above calculations are taken from the Ref. 40 and are presented in Table 1.

IV. RESULTS AND DISCUSSION

The $^{115}\text{In}(n,\gamma)^{116m}\text{In}$ reaction cross sections determined in the present work at the neutron energies of 1.12, 2.12, 3.12 and 4.12 MeV along with the literature data [14,25,26,26,28] are shown in Table 2. The uncertainties associated with the measured cross section values of the present work are from replicate measurements. The overall uncertainty is the quadratic sum of both the statistical and the systematic errors. The random error in the observed activity is primarily due to counting statistics and is estimated to be 2.1 – 6.7% for ^{116m}In . This can be determined by accumulating the data for an optimum time period that depends on the half-life of the nuclide of interest. The systematic errors are due to uncertainties in the irradiation time ($\sim 0.1\%$), the half-life of the reaction products and the γ -ray branching intensity ($\sim 2\%$), and the detection efficiency ($\sim 3\%$), which arises from the fitting error. Thus, the total systematic error is about $\sim 3.6\%$. The combined uncertainties from both the statistical and the systematic errors are 4.2 – 7.6% for the $^{115}\text{In}(n,\gamma)^{116m}\text{In}$ reaction cross section.

Table 2 shows that the $^{115}\text{In}(n,\gamma)^{116m}\text{In}$ reaction cross sections at the neutron energies of 1.12, 2.12, 3.12 and 4.12 MeV are the re-determined values and are found to be in good agreement with the literature data [14, 25,27,28]. The present data at the neutron energy of 1.12 MeV is in agreement with the data of Peto *et al.*

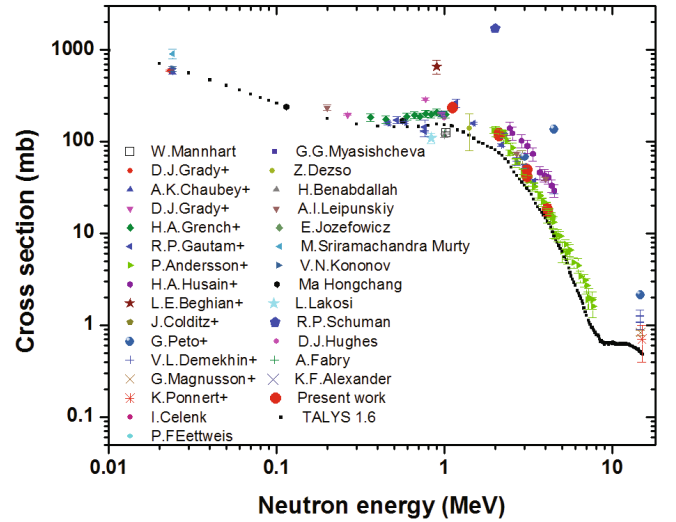


Fig. 3. (Color online) Plot of the experimental and evaluated $^{115}\text{In}(n,g)^{116m}\text{In}$ reaction cross-section data as a function of the neutron energy from 10 keV to 15 MeV. Experimental values from the present work and from Refs. 3 – 33 are in different symbols and colors, whereas the theoretical values from TALYS 1.6 are in solid squares.

[14]. Similarly, for the neutron energies of 2.12, 3.12 and 4.12 MeV, the present data are in agreement with the data of Andersson *et al.* [25,28] but lower than the values of Husain and Hunt [27]. Andersson *et al.* [25,28] experimentally determined the $^{115}\text{In}(n,\gamma)^{116m}\text{In}$ reaction cross section within the neutron energy range from 1.96 to 7.66 MeV by using the P+T and D+D neutron sources and a Ge(Li) detector. However, Husain and Hunt [27] determined the cross sections at neutron energies from 2.44 to 4.5 MeV by using the D+D neutron source and a NaI(Tl) detector. The higher values obtained by Husain and Hunt [27] are most probably due to the use of a NaI(Tl) detector or may be due to the contribution from scattered neutrons. In view of this, the $^{115}\text{In}(n,\gamma)^{116m}\text{In}$ reaction cross section as a function of the neutron energy was calculated theoretically by using the computer code TALYS version 1.6 [34] for comparison.

TALYS version 1.6 [34] can be used to calculate the reaction cross section based on physics models and parameterizations. It calculates nuclear reactions involving targets with masses larger than 12 amu and projectiles like photons, neutrons, protons, ^2H , ^3H , ^3He and alpha particles for energies up to 200 MeV. In the present work, we used the TALYS calculation for the ^{115}In target for neutron energies from 10 keV to 15 MeV by using the default values of the parameters because below neutron energy of 10 keV, resonances capture comes into play, which cannot be addressed by using the TALYS software. All possible outgoing channels for a given projectile (neutron) energy were considered, including (n, γ) and inelastic reactions. However, the (n, γ) reaction cross-sections for neutron energies from 10 keV

to 15 MeV were collected. The theoretical $^{115}\text{In}(n,\gamma)^{116m}\text{In}$ reaction cross-sections from the TALYS version 1.6 software at neutron energies of 1.12, 2.12, 3.12 and 4.12 MeV are shown in Table 2 for comparison. Table 2 shows that the experimentally-determined reaction cross sections from the present work are systematically higher than the theoretical TALYS values [34]. For comparison, the experimental data from the present work at the four neutron energies and the literature data [3–33] at other neutron energies from 10 keV to 15 MeV are plotted in Fig. 3, along with the theoretical TALYS values. Figure 3 shows that the $^{115}\text{In}(n,\gamma)^{116m}\text{In}$ reaction cross sections from the present work and the literature data [3–33] decrease with increasing neutron energy. However, the experimental data from the present work and the literature data [3–33] are slightly higher than the TALYS values but follow a similar trend. The slight difference between the experimental data and the theoretical TALYS values may be due to the use of default values of the parameters. The present data gives a guideline to an evaluator for the judgement of the literature data from earlier measurements. The $^{115}\text{In}(n,\gamma)^{116m}\text{In}$ reaction cross sections at different neutron energies from 1.5 to 10 MeV are important for its use as an alternative flux monitor to the $^{115}\text{In}(n,n')^{115m}\text{In}$ and $^{197}\text{Au}(n,\gamma)^{198g}\text{Au}$ reaction monitors. In addition, the $^{115}\text{In}(n,\gamma)^{116m}\text{In}$ reaction cross sections at different neutron energies are needed for reactor design from the point of the neutron economy of the reactor because a stable fission product such as ^{115}In is one of the symmetric fission products and are the decay products of the isobaric chain with mass number 115.

V. CONCLUSION

We determined the $^{115}\text{In}(n,\gamma)^{116m}\text{In}$ reaction cross section at neutron energies of 1.12, 2.12, 3.12 and 4.12 MeV by using an activation and off-line γ -ray spectrometric technique. Our results were found to be in good agreement with one set of the literature data, but not others. Thus, the present data gives a guideline to an evaluator for the judgement of the literature data from earlier measurements.

The $^{115}\text{In}(n,\gamma)^{116m}\text{In}$ reaction cross section as a function of the neutron energy was calculated theoretically by using the computer code TALYS version 1.6. The present data at four neutron energies and the literature data at different neutron energies are systematically higher than the values from TALYS, which may be due to the default values of the parameters.

One of the authors (B. Lawriniang) thanks the University Grant Commission (UGC) for funding in her Ph.D. work. She also thanks the staff of folded tandem ion beam accelerator (FOTIA) at Van-de-Graff, BARC and Pelletron facility, TIFR, Mumbai, for their excellent operation of the accelerator and provision of the proton beam during the irradiation.

REFERENCES

- [1] S. F. Mughabghab, M. Divadeenam and N. E. Holden, *Neutron Resonance and Thermal Cross Sections*, Vol I (Academic Press, New York, 1981).
- [2] IAEA-EXFOR Database, <http://www-nds.iaea.org/exfor>.
- [3] L. E. Beghian and H. H. Halban, *Nature (London)* **163**, 366 (1949).
- [4] D. J. Hughes, R. C. Garth and J. S. Levin, *Phys. Rev.* **91**, 1423 (1953).
- [5] D. J. Hughes, W. D. B. Spatz and N. Goldstein, *Phys. Rev.* **75**, 1781 (1949).
- [6] G. G. Myasishcheva, M. P. Anikina, L. L. Gol'din and B. V. Ershler, *Atom. Ener.* **2**, 22 (1957).
- [7] V. N. Kononov, Y. Y. Stavisskiy and V. A. Tolstikov, *Atom. Ener.* **5**, 564 (1958).
- [8] A. I. Leipunskiy, O. D. Kazachkovskiy, G. J. Artyukhov, A. I. Baryshnikov, T. S. Belanova, V. I. Galkov, Y. J. Stavisskiy, E. A. Stumbur and L. E. Sherman, *Conf. Second Internat. At. En. Conf.* (Geneva, 1958).
- [9] A. Fabry, *Nukleonik* **10**, 280 (1967).
- [10] P. Fettweis, *Phys. Lett.* **3**, 40 (1962).
- [11] K. F. Alexander and H. F. Brinckmann, *Annalen der Physik* **12**, 225 (1963).
- [12] E. Jozefowicz, *Nukleonika* **8**, 437 (1963).
- [13] A. K. Chaubey and M. L. Sehgal, *Nucl. Phys.* **66**, 267 (1965).
- [14] G. Peto, Z. Milligy and I. Hunyadi, *J. Nucl. Ener.* **21**, 797 (1967).
- [15] J. Colditz and P. Hille, *Oesterr. Akad. Wiss., Math-Naturw.Kl., Anzeiger* **105**, 236 (1968).
- [16] H. A. Grench and H. O. Menlove, *Phys. Rev.* **165**, 1298 (1968).
- [17] R. P. Schuman and R. L. Tromp, *Idaho Nuclear Corp. Reports* **1317**, 39 (1970).
- [18] Llakosi and A. Veres, *Conf. on Neutron Physics*, Kiev **4**, 312 (1973).
- [19] M. S. Murty, K. Siddappa and J. R. Rao, *J. Phys. Soc. Japan.* **35**, 8 (1973).
- [20] K. Ponnert, G. Magnusson and I. Bergqvist, *Phys. Scripta* **10**, 35 (1974).
- [21] G. Peto, J. Csikai, V. Long, S. Mukherjee, J. Banhalmi and Z. Miligy, *Acta. Phys. Slovaca* **25**, 185 (1975).
- [22] W. Mannhart, *Zeitschrift fuer Physik A, Hadrons and Nuclei* **272**, 273 (1975).
- [23] G. Magnusson and I. Bergqvist, *Nucl. Tech.* **34**, 114 (1977).
- [24] Z. Dezso and J. Csikai, *All Union Conference on Neutron Physics* (Kiev, Apr 18-22, 1977), p. 32
- [25] P. Andersson, R. Zorro and I. Bergqvist, *Conf. Nucl. Data for Sci. and Technol.* (Antwerp 1982, 1982), p. 866.
- [26] V. L. Demekhin, B. E. Leshchenko, V. K. Majdanjuk and G. Peto, *All-Union Conference on Neutron Physics* (Kiev, Oct. 2-6, 1983), p. 195.
- [27] H. A. Husain and S. E. Hunt, *Appl. Radiat. Isotopes* **34**, 731 (1983).
- [28] P. Andersson, R. Zorro, I. Bergqvist, M. Herman and A. Marcinkowski, *Nucl. Phys. A* **443**, 404 (1985).
- [29] H. Benabdallah, G. Paic and J. Csika, *Fizika* **17**, 191 (1985).
- [30] D. J. Grady, G. F. Knoll and J. C. Robertson, *Nucl. Sci. Eng.* **94**, 227 (1986).

- [31] M. Hongchang, L. Hanlin and R. Chaofan, Chinese J. Nucl. Phys. **8**, 312 (1986).
- [32] R. P. Gautam, R. K. Singh, I. A. Rizvi, M. A. Ansari, A. K. Chaubey and S. Kailas, Ind. J. Pure Appl. Phys. **28**, 235 (1990).
- [33] I. Celenk, H. Demirel and A. Ozmen, J. Radio. Nucl. Chem. **148**, 393 (1991).
- [34] A. J. Koning, TALYS user manual, A nuclear reaction program, User manual, NRG-1755 ZG PETTEN, The Netherlands (2011).
- [35] H. Naik *et al.*, Eur. Phys. J. A **47**, 51 (2011).
- [36] J. F. Ziegler, Nucl. Instrum. Methods Phys. Res. B **219-220**, 1027 (2004), available from <http://www.srim.org/>.
- [37] H. Liskien and A. Paulsen, At. Data Nucl. Data Tables **15**, 57 (1975).
- [38] C. H. Poppe, J. D. Anderson, J. C. Davis, S. M. Grimes and C. Wong, Phys. Rev. C **14**, 438 (1976).
- [39] J. W. Meadows and D. L. Smith, Neutrons from proton bombardment of natural Lithium, Argonne National Laboratory Report ANL-7983 (1972).
- [40] NuDat 2.6, National Nuclear Data Center, Brookhaven National Laboratory, updated 2011, available on <http://www.nndc.bnl.gov/>
- [41] A. T. G. Ferguson and E. B. Paul, J. Nucl. Ener. A (Reactor Science) **10**, 19(1959).
- [42] J. F. Barry, J. Nucl. Ener. A & B (Reactor Sci. and Technol.) **18**, 491 (1964).
- [43] W. Poenitz, J. Nucl. Ener. A & B (Reactor Sci. and Technol.) **20**, 825 (1966).
- [44] J. C. Robertson, T. B. Ryves, E. J. Axton, I. Goodier and A. Williams, J. Nucl. Ener. **23**, 205 (1969).
- [45] A. Paulsen, R. Widera and H. Liskien, Atomkernenergie **26**, 80 (1975).
- [46] S. K. Gupta, J. Frehaut and R. Bois, Nucl. Instrum. Methods Phys. Res. B **148**, 77 (1978).
- [47] M. B. Chadwick *et al.*, ENDF/B-VII.1: next generation evaluated nuclear data library for nuclear science and Technology, Nucl. Data Sheets **107**, 2931 (2006).
- [48] K. Shibata *et al.*, JENDL-4.0: a new library for nuclear science and engineering, J. Nucl. Sci. Tech. **48**, 1 (2011).